

# Entanglement within the Quantum Trajectory Description of Open Quantum Systems

Hyunchul Nha and H. J. Carmichael

*Department of Physics, University of Auckland, Private Bag 92019, Auckland, New Zealand*

The degree of entanglement in an open quantum system varies according to how information in the environment is read. A measure of this contextual entanglement is introduced based on quantum trajectory unravelings of the open system dynamics. It is used to characterize the entanglement in a driven quantum system of dimension  $2 \times \infty$  where the entanglement is induced by the environmental interaction. A detailed mechanism for the environment-induced entanglement is given.

PACS numbers: 03.65.Ud, 03.67.Mn, 42.50.-p

Entanglement is a remarkable feature of quantum mechanics that has attracted much attention in recent years for its potential use as a resource in quantum information processing [1]. In practical situations a quantum system inevitably couples to its environment, so that the state of the system becomes mixed. Much effort has therefore been invested in finding a reasonable measure of entanglement for mixed states. Specific proposals include the entanglement of formation [2, 3] and distillation [2], and the relative entropy of entanglement [4]. These measures are not practically computable in general, however, and are readily accessible only for low-dimensional systems [3, 4] and certain symmetric states [5]. Recently, a variational method for calculating the entanglement of formation (EOF) in general bipartite states was developed [6]. For bipartite mixed states, a computable measure of entanglement based on the negativity of the partial transpose has also been proposed [7]. In the case of continuous variable systems, the EOF of symmetric two-mode Gaussian states was recently obtained [8].

In this Letter we consider mixed state entanglement from a new perspective. For pure states, the accepted measure of entanglement is settled. Considering a bipartite state  $\rho_i = |\psi_i\rangle\langle\psi_i|$  (subsystems  $A$  and  $B$ ), it is calculated as the von Neumann entropy

$$E(\rho_i^B) = -\text{tr}_B[\rho_i^B \log_2(\rho_i^B)], \quad (1)$$

where  $\rho_i^B = \text{tr}_A(|\psi_i\rangle\langle\psi_i|)$  [2]. It is well known that any mixed state  $\rho$  may be decomposed into an ensemble of pure states in an infinity of ways:  $\rho = \sum_i p_i |\psi_i\rangle\langle\psi_i|$ , where  $p_i \geq 0$  and  $\sum_i p_i = 1$ . Given a decomposition, the entanglement may be quantified by the ensemble average  $E = \sum_i p_i E(\rho_i^B)$ . The perceived difficulty here is with the arbitrariness of the decomposition. Measures of mixed state entanglement differ in their strategy for replacing this arbitrariness by something specific. The EOF, for example, is defined as the minimum over all decompositions; it intends to quantify the resources required to produce the state  $\rho$  under a specified quantum communication protocol [2, 3]. The work reported in this Letter takes a different view. We observe that entangled states are pervasive in the quantum mechanics of composite systems, often arising in situations that have no immediate quantum information connection. With the aim of understanding entanglement in this broader sense, we propose

to explore, rather than discard, the multiplicity of mixed state decompositions. The ambiguity arising in the multiplicity is viewed as a signature of complementarity, i.e., an expected feature that reflects the very essence of a quantum mechanical description.

We consider entanglement in bipartite open systems, specifically, where we resolve the arbitrariness in the decomposition of  $\rho$  by limiting attention to physically relevant decompositions—those for which  $p_i$  is the probability of a classical record comprising information read from the environment. This information may be read in many ways. For each, there is a different decomposition of  $\rho$  and hence a different degree of entanglement. Quantum trajectory theory [9] provides a natural measure of this entanglement in the form

$$E_U = \overline{E(\rho_{U;\text{REC}}^B)}, \quad (2)$$

with  $\rho_{U;\text{REC}}^B = \text{tr}_A(|\psi_{U;\text{REC}}\rangle\langle\psi_{U;\text{REC}}|)$ , where  $U$  labels a particular unraveling of the open system dynamics (reading of the environment) and REC denotes a particular record; the overbar in Eq. (2) denotes an average over records. The reading of the environment is continuous in time, and to preserve the purity of the state  $|\psi_{U;\text{REC}}\rangle$ , 100% efficient (all scattered particles are ultimately detected).  $E_U$  has a particular significance for each physically realizable unraveling.

We explore these ideas in an example, where we characterize the entanglement in a composite system consisting of ( $A$ ) an optical cavity mode (harmonic oscillator), resonantly coupled to ( $B$ ) a two-state atom (single qubit). The atom is driven by a resonant external field and both subsystems are coupled to Markov reservoirs to account for the scattering of light into the vacuum of the electromagnetic field. The Hamiltonian is

$$H = H_{AB} + H_{\text{ext}}^B + H_{\text{res}}, \quad (3)$$

with

$$\begin{aligned} H_{AB} &= \hbar\omega(\hat{a}^\dagger\hat{a} + \hat{b}^\dagger\hat{b}) + i\hbar g(\hat{a}^\dagger\hat{b} - \hat{b}^\dagger\hat{a}), \\ H_{\text{ext}}^B &= i\hbar\Omega(\hat{b}^\dagger e^{-i\omega t} - \hat{b} e^{i\omega t}), \\ H_{\text{res}} &= H_{RA} + H_{RB} + H_{RA} + H_{BRB}, \end{aligned} \quad (4)$$

where  $\hat{a}$  and  $\hat{a}^\dagger$  are cavity mode annihilation and creation operators ( $[\hat{a}, \hat{a}^\dagger] = 1$ ), and  $\hat{b}$  and  $\hat{b}^\dagger$  are lowering and

raising operators for the atom ( $[\hat{b}, \hat{b}^\dagger]_+ = 1$ ). The external field has amplitude  $\Omega$ , and  $A$  and  $B$  couple to reservoirs  $R_A$  and  $R_B$ , respectively, via interactions  $H_{AR_A}$  and  $H_{BR_B}$ . The evolution of the reduced density operator  $\tilde{\rho}$  in the interaction picture is governed by the master equation

$$\frac{d\tilde{\rho}}{dt} = \frac{1}{i\hbar}[\tilde{H}_{AB} + \tilde{H}_{\text{ext}}^B, \tilde{\rho}] + (\mathcal{L}_A + \mathcal{L}_B)\tilde{\rho}, \quad (5)$$

where  $\tilde{H}_{AB} = i\hbar(\hat{a}^\dagger\hat{b} - \hat{b}^\dagger\hat{a})$ ,  $\tilde{H}_{\text{ext}}^B = i\hbar\bar{\Omega}(\hat{b}^\dagger - \hat{b})$ , with  $\bar{\Omega} \equiv \Omega/g$ ,  $\bar{t} \equiv gt$ , and

$$\mathcal{L}_{A,B} = \bar{\Gamma}_{a,b}(2\hat{o} \cdot \hat{o}^\dagger - \hat{o}^\dagger\hat{o} \cdot \dots \hat{o}^\dagger\hat{o}), \quad (6)$$

where  $(\hat{o} = \hat{a}, \hat{b})$  and the damping constants  $\bar{\Gamma}_{a,b} \equiv \Gamma_{a,b}/g$  determine the reservoir interaction strengths.

The dimension of  $A \otimes B$  is  $2 \times \infty$ ; hence the results of Refs. [4, 5, 6, 8] do not apply. The system exhibits the additional interesting feature of *environment-assisted entanglement*—i.e., an interaction with the environment is required to generate entanglement. Specifically, the degree of entanglement increases with the damping of the cavity mode  $A$ , passes through a peak, and then decreases again. The behavior illustrates something of the subtlety associated with entanglement generation in open systems; the environment is not simply a source of decoherence. Squeezing in the considered system shows a similar counterintuitive dependence on the cavity damping [10]. Entanglement generation through an environmental interaction has also been reported for two cavity modes coupled to an incoherently driven atom [11] and for two atoms coupled to a common bath [12].

We first uncover the origin of the environment-assisted entanglement. We note that  $\tilde{H}_{AB} + \tilde{H}_{\text{ext}}^B$  has an eigenstate  $|\alpha\rangle|g\rangle$ ,  $\alpha = \bar{\Omega}$ , where  $|\alpha\rangle$  is a coherent state of  $A$  and  $|g\rangle$  denotes the ground state of  $B$ . The interpretation is that since the atom interacts with the sum of fields  $\hat{a} - \bar{\Omega}$ , it is stable in its ground state if the summed field amplitude is zero. In the presence of damping  $\bar{\Gamma}_b \neq 0$ , but with  $\bar{\Gamma}_a = 0$ , this eigenstate becomes the system steady state (a *dark state*) for all  $\bar{\Gamma}_b$  and  $\bar{\Omega}$  [13]. Thus, if there is no interaction between subsystem  $A$  and its environment the system steady state is the product state  $|\bar{\Omega}\rangle|g\rangle$ , and the entanglement  $E_U$  is zero; effectively the coupling between subsystems is turned off. The environmental interaction  $\bar{\Gamma}_a$  destabilizes the dark state, restores the coupling, and generates entanglement.

To describe the situation for  $\bar{\Gamma}_a \neq 0$  it is convenient to introduce the displaced state  $\tilde{\rho}'$ , with  $\tilde{\rho} = \hat{D}^\dagger(\bar{\Omega})\tilde{\rho}'\hat{D}(\bar{\Omega})$ , where  $\hat{D}(\bar{\Omega}) \equiv \exp[\bar{\Omega}(\hat{a}^\dagger - \hat{a})]$ . Since  $\hat{D}(\bar{\Omega})$  is a local unitary operator, it does not change the degree of entanglement. The displacement moves the driving from  $B$  to  $A$  [14]. In place of Eq. (5), we obtain

$$\frac{d\tilde{\rho}'}{dt} = \frac{1}{i\hbar}[\tilde{H}_{AB} + \tilde{H}_{\text{ext}}^A, \tilde{\rho}'] + (\mathcal{L}_A + \mathcal{L}_B)\tilde{\rho}', \quad (7)$$

where  $\tilde{H}_{\text{ext}}^A = i\hbar\bar{\Gamma}_a\bar{\Omega}(\hat{a} - \hat{a}^\dagger)$ . Note that  $\bar{\Gamma}_a$  appears in two places: in the driving field interaction  $\tilde{H}_{\text{ext}}^A$ , where

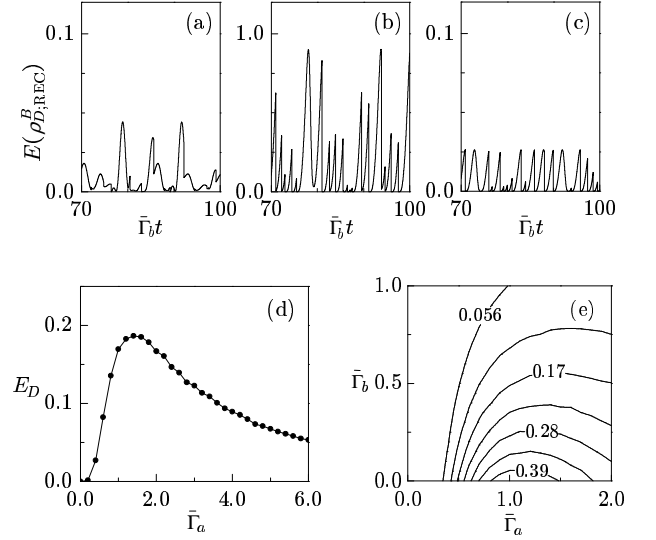


FIG. 1: Entanglement in direct detection, for  $\bar{\Omega} = 1$ : typical temporal behavior of the von Neumann entropy for  $\bar{\Gamma}_b = 0.5$  and  $\bar{\Gamma}_a = 0.3$  (a), 2.0 (b), and 20.0 (c); (d) entanglement [Eq. (2)] as a function of  $\bar{\Gamma}_a$  (for  $\bar{\Gamma}_b = 0.5$ ); (e) entanglement as a function of  $\bar{\Gamma}_a$  and  $\bar{\Gamma}_b$ .

it governs the described creation of entanglement, and in the usual damping term  $\mathcal{L}_A\tilde{\rho}'$ . The interplay of the two, along with the interaction  $\tilde{H}_{AB}$ , determines the behavior of the entanglement as a function of  $\bar{\Gamma}_a$ . In particular, in the limit  $\bar{\Gamma}_a \rightarrow \infty$ , the steady state of the cavity field in the displaced frame balances  $\tilde{H}_{\text{ext}}^A$  with  $\mathcal{L}_A$ . This yields a coherent state of amplitude  $\alpha' = -\bar{\Omega}$ , the vacuum state in the original frame (see Fig. 2). Thus, in the large  $\bar{\Gamma}_a$  limit, the steady state approaches  $\tilde{\rho} = \tilde{\rho}_A\tilde{\rho}_B$ , where  $\tilde{\rho}_A = |0\rangle\langle 0|$  and  $\tilde{\rho}_B$  is determined by the balancing of  $\tilde{H}_{\text{ext}}^B$  with  $\mathcal{L}_B$ , i.e.,  $\tilde{\rho}_B$  is the steady state of resonance fluorescence. In summary, for  $\bar{\Gamma}_a = 0$  or  $\infty$  the entanglement is zero.

Consider now the quantification of entanglement in between these limits. Figure 1 illustrates the behavior with the unraveling of the density operator based upon direct detection of the scattered photons (unraveling  $U = D$ ), those scattered through the cavity mirrors via the coupling of  $B$  to  $A$  and those scattered directly by the atom  $B$ . Frames (a)-(c) illustrate the time dependence of the von Neumann entropy, where the entanglement is conditioned on a particular record of photon counts. Frames (d) and (e) show results after taking the average over records (a time average is permitted since trajectories are ergodic [15, 16]). In the small and large damping limits, the entanglement is calculated to be

$$E_D = -\lambda \log_2 \lambda - (1 - \lambda) \log_2 (1 - \lambda), \quad (8)$$

with  $\lambda \approx \bar{\Omega}^4 \bar{\Gamma}_a^6$  and  $\lambda \approx (2/\bar{\Gamma}_a)^2 (4\bar{\Omega}/\bar{\Gamma}_b)^4$ , respectively. The peak in between these limits is shown in Figs. 1(d) and (e), and is to be compared with the monotonic decrease of  $E_D$  with increasing  $\bar{\Gamma}_b$ . (Increasing  $\bar{\Gamma}_b$  increases the rate of interruptions, due to the detection of a photon in the environment, that return the atom to the ground

state; each interruption destroys any entanglement created since the previous photon detection.)

We turn now to the variation in the degree of entanglement for different unravelings ( $U$ ) of  $\rho$ . For simplicity, we set  $\bar{\Gamma}_b = 0$  and focus attention on the behavior of the entanglement as a function of  $\bar{\Gamma}_a$ . We begin by presenting an analytical approximation, which clarifies the behavior in Fig. 1(d) and serves as an introduction to the unraveling-dependence of the entanglement.

Alsing and Carmichael [14] performed a semiclassical analysis of Eq. (7). They found that as a function of the parameter  $\xi \equiv (2\bar{\Gamma}_a\bar{\Omega})^{-1}$ , the composite system exhibits a symmetry breaking transition at  $\xi = 1$  (spontaneous dressed state polarization). If  $\alpha = \bar{\Omega}(x + iy)$  and  $\beta = u + iv$  denote complex amplitudes of the cavity field and atomic polarization, in steady state

$$\begin{aligned} \alpha/\bar{\Omega} &= 1, \quad \beta = 1/\xi, & (\xi \geq 1), \\ \alpha_{\pm}/\bar{\Omega} &= \xi\beta_{\pm} = \xi \left[ \xi \pm i\sqrt{1-\xi^2} \right], & (\xi \leq 1). \end{aligned} \quad (9)$$

Figures 2(a) and (b) illustrate the behavior of the steady-state amplitudes as a function of  $\bar{\Gamma}_a$ . For  $\bar{\Gamma}_a > 1/2\bar{\Omega}$  ( $\xi < 1$ ), there are two permissible values for the amplitude of  $A$ , each correlated with an amplitude for  $B$ . With increasing  $\bar{\Gamma}_a$ , the amplitudes of  $A$  separate and move in opposite directions on a circle of radius  $\bar{\Omega}/2$ ; they reach maximum separation at  $\bar{\Gamma}_a = 1/\sqrt{2}\bar{\Omega}$  and approach one another on the opposite side of the circle for  $\bar{\Gamma}_a \gg 1$ . The correlated amplitudes of  $B$  move on a semicircle as

shown. If  $\bar{\Omega} \gg 1$ , the phase-space separation across the circle is large compared with the vacuum-state uncertainty of oscillator  $A$  [point (3) in Fig. 2(a)]. In such a case, the Wigner function for the reduced quantum-mechanical steady state  $\tilde{\rho}_A = \text{tr}_B(\tilde{\rho})$  is double peaked, as shown in Fig. 2(c).

The full quantum-mechanical steady state  $\tilde{\rho}$  is approximated, for  $\bar{\Omega} \gg 1$ , by an equally weighted mixture of the states  $|\alpha_+\rangle|\beta_+\rangle$  and  $|\alpha_-\rangle|\beta_-\rangle$ , where  $|\alpha_{\pm}\rangle$  are coherent states of oscillator  $A$  and the states of  $B$  are  $|\beta_{\pm}\rangle = (\sqrt{\beta_{\pm}}|e\rangle + \sqrt{\beta_{\pm}^*}|g\rangle)/\sqrt{2}$ , where  $|e(g)\rangle$  denotes the excited (ground) state of the atom. Two compatible pure state ensembles are

$$|\psi_{\text{REC}}\rangle = \Theta_{\text{REC}}|\alpha_+\rangle|\beta_+\rangle + (1 - \Theta_{\text{REC}})|\alpha_-\rangle|\beta_-\rangle, \quad (10)$$

with  $\Theta_{\text{REC}} = 0, 1$  a dichotomous random variable (probabilities  $p_0 = p_1 = 1/2$ ), and

$$|\psi_{\text{REC}}\rangle = N(e^{i\Phi_{\text{REC}}}|\alpha_+\rangle|\beta_+\rangle + e^{-i\Phi_{\text{REC}}}|\alpha_-\rangle|\beta_-\rangle), \quad (11)$$

with  $\Phi_{\text{REC}}$  uniformly distributed between 0 and  $\pi$ . For ensemble (10) the entanglement  $E_U$  is zero; therefore the approximate  $\tilde{\rho}$  is separable. Nevertheless, the von Neumann entropy of state (11) is nonzero. We find it may be computed from Eq. (8) by replacing  $\lambda$  with

$$\lambda_{\pm}(\Phi_{\text{REC}}) = \frac{1}{2} \pm \frac{1}{2} \frac{\sqrt{A^2(\Phi_{\text{REC}}) + B^2(\Phi_{\text{REC}})}}{B(\Phi_{\text{REC}})}, \quad (12)$$

where

$$A(\Phi_{\text{REC}}) = \sqrt{1 - \xi^2} e^{-2\bar{\Omega}^2 y^2} \sin[2(\bar{\Omega}^2 xy + \Phi_{\text{REC}})], \quad (13)$$

$$B(\Phi_{\text{REC}}) = \xi + e^{-2\bar{\Omega}^2 y^2} \cos[2(\bar{\Omega}^2 xy + \Phi_{\text{REC}})]. \quad (14)$$

After averaging over records a nonzero entanglement is obtained. It is plotted as the dashed curve in Fig. 3(b), where the behavior as a function of  $\bar{\Gamma}_a$  resembles that in Fig. 1(d), except Fig. 3(b) shows a higher peak, approaching unity for  $\bar{\Omega} \gg 1$ . Clearly there is a vast difference in the entanglement computed for ensembles (10) ( $E_U = 0$ ) and (11) ( $E_U \approx 1$ ).

The difference has a physical origin; it arises from the way in which information is read from the environment. Ensemble (10) yields  $E_U = 0$  because it assumes that this information—encoded in  $\Theta_{\text{REC}}$ —is able to distinguish between  $|\alpha_+\rangle$  and  $|\alpha_-\rangle$ . Ensemble (11) assumes the opposite—that the record read in the environment cannot distinguish between  $|\alpha_+\rangle$  and  $|\alpha_-\rangle$ . Direct detection of scattered photons cannot distinguish these states, for example, because  $|\alpha_+|^2 = |\alpha_-|^2$ . Neither can measuring the amplitude  $\text{Re}(\alpha_+) = \text{Re}(\alpha_-)$ . Measuring  $\text{Im}(\alpha_+) = -\text{Im}(\alpha_-)$ , on the other hand, can.

More generally, let us define the quadrature amplitude  $\hat{X}_{\theta} = (e^{i\theta}\hat{a}^{\dagger} + e^{-i\theta}\hat{a})/2$  and consider the homodyne detection unraveling of  $\tilde{\rho}$  (in the strong local oscillator limit;  $U = H$ ) corresponding to a  $\theta$ -quadrature measurement of the light scattered into reservoir  $R_A$ . The pure

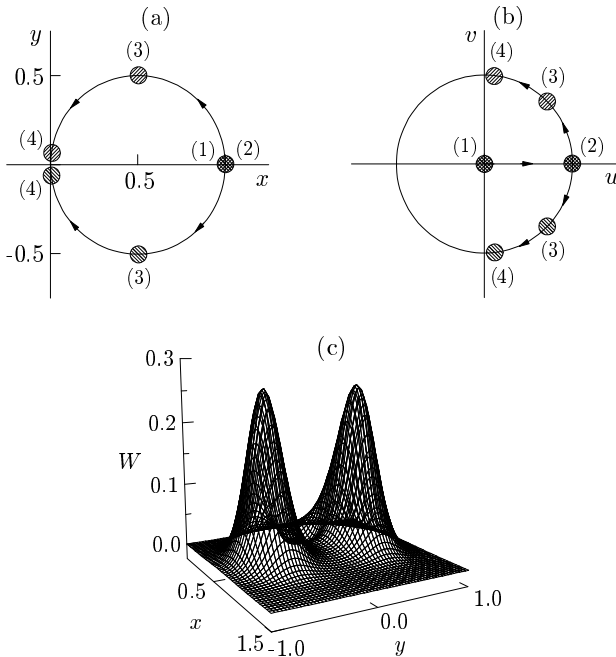


FIG. 2: Behavior of the semiclassical steady-state amplitudes  $\alpha/\bar{\Omega}$  (a) and  $\beta$  (b) [Eq. (9)] with increasing  $\bar{\Gamma}_a$ ; the labeled points are (1)  $\bar{\Gamma}_a = 0$ , (2)  $\bar{\Gamma}_a = 1/2\bar{\Omega}$ , (3)  $\bar{\Gamma}_a = 1/\sqrt{2}\bar{\Omega}$ , and (4)  $\bar{\Gamma}_a \gg 1$ . (c) Steady-state Wigner function for  $\bar{\Gamma}_a = 1/\sqrt{2}\bar{\Omega}$  (maximum peak separation) for  $\bar{\Omega} = 3$ .

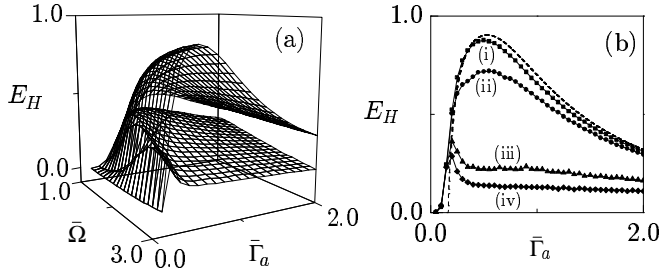


FIG. 3: Entanglement in homodyne detection: (a) as a function of  $\bar{\Gamma}_a$  and  $\bar{\Omega}$  for  $\theta = 0$  (upper surface) and  $\theta = \pi/2$  (lower surface); (b) for fixed  $\bar{\Omega} = 3$  and (i)  $\theta = 0$ , (ii)  $\theta = \pi/40$ , (iii)  $\theta = \pi/10$ , and (iv)  $\theta = \pi/2$ , the dashed line is the entanglement in ensemble (11). All results are for  $\bar{\Gamma}_b = 0$ .

state ensemble is generated in this case by the stochastic Schrödinger equation [9]

$$d|\bar{\psi}_{\text{REC}}\rangle = \left( \frac{1}{i\hbar} \tilde{H}_{\text{eff}} d\bar{t} + e^{-i\theta} \sqrt{2\bar{\Gamma}_a} \hat{a} d\bar{q}_\theta \right) |\bar{\psi}_{\text{REC}}\rangle, \quad (15)$$

where  $\tilde{H}_{\text{eff}} \equiv \tilde{H}_{AB} + \tilde{H}_{\text{ext}}^B - \bar{\Gamma}_a \hat{a}^\dagger \hat{a}$ , and

$$d\bar{q}_\theta = \sqrt{2\bar{\Gamma}_a} \langle e^{i\theta} \hat{a} + e^{-i\theta} \hat{a}^\dagger \rangle_{\text{REC}} d\bar{t} + d\bar{W} \quad (16)$$

is the record of charge deposited in the detector;  $d\bar{W}$  is a real Wiener increment. Results for  $E_H$  are displayed in Fig. 3. In Fig. 3(a) we plot the maximum and minimum values of  $E_H$  obtained with  $\theta = 0$  and  $\pi/2$ , respectively, as a function of  $\bar{\Omega}$  and  $\bar{\Gamma}_a$ . The minimum provides an upper bound on the EOF. It is not zero as in ensemble (10) because  $\bar{\Omega}$  is finite. In Fig. (3)(b), the maximum  $E_H$  is well-approximated by Eqs. (12)-(14) even for  $\bar{\Omega} = 3$ .

The optimal entanglement occurs along a curve with  $\bar{\Omega}$  inversely proportional to  $\bar{\Gamma}_a$ , which is what one would expect from the definition of points (2) and (3) in Fig. 2. Note, however, that with  $\bar{\Omega}$  fixed, the peak, as a function of  $\bar{\Gamma}_a$ , does not occur where  $|\alpha_+\rangle$  and  $|\alpha_-\rangle$  are maximally separated in phase space. This is explained by  $|\beta_+\rangle$  and  $|\beta_-\rangle$ , which are not orthogonal at maximum separation, but only approach orthogonality as  $\bar{\Gamma}_a \rightarrow \infty$ .

Returning to our general theme, existing measures of entanglement view a mixed state  $\rho$  as a fundamental object and aim to associate a unique number with  $\rho$ . For open composite systems the mixing arises from a well-defined process. In this case, more can be said about entanglement by considering how the system acts upon its environment—nonlocally in the case of emitted light. Entanglement, as with the correlations it describes, becomes a contextual notion. In this Letter we have shown how quantum trajectory theory can quantify such entanglement, capturing the context-dependence in its different unravelings of  $\rho$ .

Many questions are left open concerning observable ramifications of  $E_U$  for different unravelings  $U$ . When the environment is monitored as a means of conditional state preparation [17], physical implications are clear. More generally, do the records themselves contain indications that the system generating the measured outputs is described by an entangled state? The sensitivity of  $E_U$  to minor changes in record making (imperfect detection) is also an interesting topic, with implications for decoherence theory and the classical limit. These and other issues are left for future investigation.

This work was supported by the NSF under Grant No. PHY-0099576 and by the Marsden Fund of the RSNZ.

- 
- [1] M. A. Nielsen and I. L. Chuang, *Quantum Computation and Quantum Information* (Cambridge University Press, Cambridge, 2000).
  - [2] C. H. Bennett *et al.*, Phys. Rev. A **54**, 3824 (1996).
  - [3] W. K. Wootters, Phys. Rev. Lett. **80**, 2245 (1998).
  - [4] V. Vedral *et al.*, Phys. Rev. Lett. **78**, 2275 (1997); V. Vedral *et al.*, Phys. Rev. A **57**, 1619 (1998).
  - [5] B. M. Terhal, and K. G. H. Vollbrecht, Phys. Rev. Lett. **85**, 2625 (2000).
  - [6] K. Audenaert *et al.*, Phys. Rev. A **64**, 052304 (2001).
  - [7] G. Vidal and R. F. Werner, Phys. Rev. A **65**, 32314 (2002).
  - [8] G. Giedke *et al.*, Phys. Rev. Lett. **91**, 107901 (2003).
  - [9] H. J. Carmichael, *An Open Systems Approach to Quantum Optics*, Lecture Notes in Physics, New Series m: Monographs, Vol. m18 (Springer-Verlag, Berlin, 1993).
  - [10] H. Nha, Phys. Rev. A **67**, 23801 (2003).
  - [11] M. B. Plenio and S. F. Huelga, Phys. Rev. Lett. **88**, 197901 (2002).
  - [12] F. Bennati *et al.*, Phys. Rev. Lett. **91**, 070402 (2003).
  - [13] P. Alsing *et al.*, Phys. Rev. A **45**, 1793 (1992).
  - [14] P. Alsing and H. J. Carmichael, Quantum Opt. **3**, 13 (1991).
  - [15] B. Kümmerer and H. Maassen, J. Phys. A **36**, 2155 (2003).
  - [16] J. D. Cresser, in *Directions in Quantum Optics*, edited by H. J. Carmichael *et al.* (Springer-Verlag, Berlin, 2001), p. 358.
  - [17] S. Bose *et al.*, Phys. Rev. Lett. **24**, 5158 (1999).